Eur. Phys. J. D **30**, 279–285 (2004)
DOI: 10.1140/epjd/e2004-00090-6

THE EUROPEAN PHYSICAL JOURNAL D

Non-linear and quantum optics of a type II OPO containing a birefringent element

1. Classical operation

L. Longchambon, J. Laurat, T. Coudreau[a], and C. Fabre

Laboratoire Kastler Brossel, Case 74, UPMC, 4 place Jussieu, 75252 Paris Cedex 05, France

Received 6 October 2003 / Received in final form 12 February 2004
Published online 23 July 2004

Abstract. We describe theoretically the main characteristics of the steady state regime of a type II Optical Parametric Oscillator (OPO) containing a birefringent plate. In such a device the signal and idler waves are at the same time linearly coupled by the plate and nonlinearly coupled by the $\chi^{(2)}$ crystal. This mixed coupling allows, in some well-defined range of the control parameters, frequency degenerate operation as well as phase locking between the signal and idler modes. We describe here a complete model taking into account all possible effects in the system, i.e. arbitrary rotation of the waveplate, non perfect phase matching, ring and linear cavities. This model is able to explain the detailed features of the experiments performed with this system.

PACS. 42.65.-k Nonlinear optics – 42.65.Yj Optical parametric oscillators and amplifiers – 42.60.Fc Modulation, tuning, and mode locking – 42.25.Lc Birefringence

1 Introduction

In a type II OPO, signal and idler fields of crossed polarizations are generated when the pump exceeds a certain threshold. Energy conservation requires that $\omega_0 = \omega_1 + \omega_2$, where ω_0, ω_1 and ω_2 are respectively the pump, signal and idler frequencies. The precise values of the signal and idler frequencies are set by the conditions of equal cavity detunings and minimum oscillation threshold, which depend on the value of the phase matching between the three waves, and on the vicinity of cavity resonances for the signal and idler modes. Theses frequencies are determined unambiguously when one knows the values of two control parameters of the OPO, namely the crystal temperature (which sets the value of the different indices) and the cavity length (which determines the cavity resonance conditions). Frequency degeneracy, i.e. $\omega_1 = \omega_2 = \omega_0/2$, occurs only accidentally since it corresponds to a single point in the parameter space. It cannot be achieved for a long time in real experimental conditions, as these parameters drift in time. Furthermore, even when the device is actively stabilized on the frequency degeneracy working point, the signal and idler fields still undergo a phase diffusion phenomenon, similar to the Schawlow-Townes effect in a laser [1,2], but acting on the difference between the phases of the signal and idler modes in the case of the type II OPO. As a result, the output field polarization direction slowly drifts with time.

In the context of quantum information and generation of EPR correlated bright beams, where both amplitude and phase correlations are involved, phase locking is interesting since it allows a much simpler measurement of amplitude *and* phase quantum correlations between the signal and idler beams [3] even above threshold: the measurement of intensity quantum correlations between the signal and idler modes can be done even with non-frequency degenerate beams [4] but the measurement of phase correlations makes it necessary to use a local oscillator. Thus a phase reference is defined and signal and idler must be stable compared to this reference, which is not the case in a regular, above threshold, type II OPO.

A few years ago, Wong et al. had the idea of achieving the frequency degenerate operation at the output of a type-II OPO by introducing a linear coupling between the signal and idler fields. This coupling was made by way of a birefringent quarter-wave plate placed inside the OPO linear cavity which couples the two orthogonally polarized signal and idler waves. In this way, they generated intense and stable frequency degenerate signal and idler beams [5]. The theoretical model described in reference [6] was able to account for the main features of this phenomenon, but, for the sake of simplicity, it was made for a ring cavity, for a small angle between the crystal neutral axes and the

[a] e-mail: coudreau@spectro.jussieu.fr

birefringent plate neutral axes, and without any phase-shifts introduced by the reflection on the cavity mirrors or by non perfect phase matching.

Most experiments use linear cavities, whereas most theoretical treatments assume ring cavities. For scalar fields there is almost no difference between the two configurations (the crystal in the ring cavity being taken twice as long as the linear cavity), if one neglects the cavity mirror differential phase-shifts. This is no longer the case when polarization effects are taken into account: in this case, a matrix formalism is needed, and the exact succession of the different elements in the cavity is now important, as they are described by non-commuting matrices. It is also interesting to examine the regime when the birefringent plate angle is not limited to small values. It seems also important to take into account the mirror phase shifts, which are known to induce a significant change in the phase matching between the three waves and consequently in the oscillation threshold of the linear cavity OPO [7]. The purpose of the present paper is to introduce all these refinements in the theoretical model introduced in [6], and also to discuss the properties of the phase-locked OPO in terms of the actual control parameters of the device, which are the cavity length and the crystal temperature. This paper is followed by a second one [3] in which the quantum fluctuations and correlations between the signal and idler fields are determined and studied in the same configuration.

In Section 2, we introduce and describe the behavior of the different elements placed inside the OPO cavity. We then determine and discuss in Section 3 the steady-state regime in the ring cavity case. Finally, in Section 4, we examine and discuss the steady state regime in the linear cavity case.

2 Linear and nonlinear elements in the OPO cavity

We consider here a $\chi^{(2)}$ crystal with a type II phase matching, which means that the signal and idler fields have orthogonal polarizations. The crystal length is l and its indices of refraction are n_1 and n_2 respectively for the signal (ordinary) and idler (extraordinary) waves which are supposed to be frequency degenerate. The non degenerate case will be studied elsewhere [8].

Assuming a small variation of the various field amplitudes inside the nonlinear medium, which is quite reasonable in a c.w. OPO, one can solve in an approximate way the propagation equations inside the crystal, and obtain to the second order in the non-linearity, g:

$$A_0(l) = A_0(0) - g\exp\left(-i\frac{\Delta kl}{2}\right)\mathrm{sinc}\left(\frac{\Delta kl}{2}\right)A_1(0)A_2(0) - \frac{g^2}{2}f^*\left(\frac{\Delta kl}{2}\right)\left(|A_1(0)|^2 + |A_2(0)|^2\right)A_0(0)$$

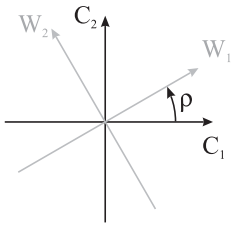

Fig. 1. ρ is the angle between the crystal's axes ((C_1, C_2), black lines) and the waveplate axes ((W_1, W_2), grey lines).

$$\begin{aligned}A_1(l) &= A_1(0) + g\exp\left(i\frac{\Delta kl}{2}\right)\mathrm{sinc}\left(\frac{\Delta kl}{2}\right)A_0(0)A_2^*(0) \\ &\quad + \frac{g^2}{2}f\left(\frac{\Delta kl}{2}\right)\left(|A_0(0)|^2 - |A_2(0)|^2\right)A_1(0) \\ A_2(l) &= A_2(0) + g\exp\left(i\frac{\Delta kl}{2}\right)\mathrm{sinc}\left(\frac{\Delta kl}{2}\right)A_0(0)A_1^*(0) \\ &\quad + \frac{g^2}{2}f\left(\frac{\Delta kl}{2}\right)\left(|A_0(0)|^2 - |A_1(0)|^2\right)A_2(0) \qquad (1)\end{aligned}$$

in which A_0 is the envelope amplitude of the pump field and the A_i, $i = 1, 2$ are the envelope amplitudes of the down converted fields, assumed to be plane waves, along the crystal axes (C_1: ordinary wave, C_2: extraordinary wave); the envelopes are normalized in such a way that $|A_i|^2$ gives the photon flow (photon $\mathrm{m}^{-2}\,\mathrm{s}^{-1}$); g is the nonlinear coupling coefficient given by

$$g = l\chi^{(2)}\sqrt{\frac{\hbar\omega_0\omega_1\omega_2}{2c^3\varepsilon_0 n_0 n_1 n_2}} \qquad (2)$$

and $f(x) = \exp(ix)(\exp(ix) - \mathrm{sinc}(x))/ix$. The crystal input-output equations are then, when one expresses the pump field at the center of the crystal:

$$\begin{aligned}A_1(l) &= A_1(0) + g'A_0\left(\frac{l}{2}\right)A_2^*(0) \\ A_2(l) &= A_2(0) + g'A_0\left(\frac{l}{2}\right)A_1^*(0) \qquad (3)\end{aligned}$$

where $g' = g\exp(i\Delta kl/2)\,\mathrm{sinc}\,(\Delta kl/2)$. The advantage of this expression is that it is valid to the second order in the non-linearity g'.

The second element in the cavity is the birefringent wave plate. It has a thickness e and its indices of refraction are n_e and n_f at frequency $\omega_0/2$ respectively for the slow and fast axes which make an angle ρ with the crystal axes (see Fig. 1).

Its effect will be described in the Jones matrices formalism [9] in the nonlinear crystal axes basis. The transmission through the wave plate can be written as the matrix:

$$M = e^{ikne}\begin{pmatrix}\alpha & \epsilon \\ \epsilon & \alpha^*\end{pmatrix} \qquad (4)$$

where

$$n = \frac{n_s + n_f}{2} \qquad (5)$$

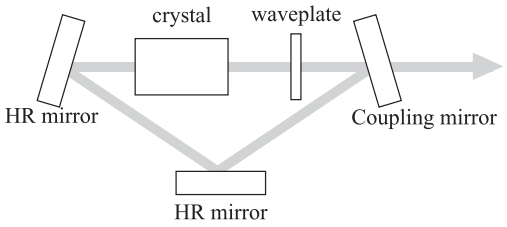

Fig. 2. Set-up of the ring cavity; we consider only one direction of propagation.

represents the mean index of refraction of the waveplate, and

$$\alpha = \cos\left(\frac{\Delta\phi}{2}\right) + i\cos(2\rho)\sin\left(\frac{\Delta\phi}{2}\right) \tag{6}$$

$$\epsilon = i\sin\left(\frac{\Delta\phi}{2}\right)\sin(2\rho) \tag{7}$$

where $\Delta\phi = k(n_s - n_f)e$ is the waveplate birefringent phase-shift. Let us set $\alpha = \alpha_0 e^{i\psi}$ where $(\alpha_0, \psi) \in \mathbb{R}^2$. For the sake of simplicity, we will assume that this plate has no effect on the pump field polarization, i.e. acts as a λ waveplate at the pump frequency.

3 Ring cavity type II OPO

We assume in this section that the cavity has a ring shape (Fig. 2), and that the coupling mirror has large reflection coefficients for signal and idler modes (r_1 and r_2). The moduli of the amplitude reflection coefficients of the coupling mirror are taken equal for the signal and idler modes: $|r_1| = |r_2| = r = 1 - \kappa$, with $\kappa \ll 1$, so that the transmission is $|t| \approx \sqrt{2\kappa}$. μ is the round-trip loss coefficient for the signal and idler waves (due to crystal absorption, surface scattering, other mirror finite transmission...), assumed to be small. We define a generalized reflection coefficient: $r' = r(1-\mu) \approx 1 - (\mu + \kappa)$. We will call ζ_1 and ζ_2 the phase-shifts introduced by the reflection on the cavity mirrors for the signal and idler waves so that $r_j = r\exp(i\zeta_j)$, $j = 1, 2$. In all the article, we do not take into account the resonance of the pump mode: all equations are given for the pump field inside the crystal and we only calculate operating thresholds (not signal or idler intensities) normalized to the intracavity pump threshold of the OPO without the waveplate (standard OPO threshold), σ_0. The free propagation length inside the cavity is denoted L.

As the signal and idler fields are assumed to have the same frequency, the birefringent plate and the non-linear crystal couple the same fields, which are the ordinary and extraordinary waves at frequency $\omega_0/2$, and only three complex equations are needed to describe the system. From equations (3) and (4), one readily obtains the following steady state equations for the field amplitudes $A_1 = A_1(0)$ and $A_2 = A_2(0)$:

$$\begin{aligned} A_1 &= r'\alpha_0 e^{i(\delta-\theta/2+\psi)}\left(A_1 + g' A_0 A_2^*\right) \\ &\quad + r'\epsilon e^{i(\delta+\theta/2)}\left(A_2 + g' A_0 A_1^*\right) \\ A_2 &= r'\alpha_0 e^{i(\delta+\theta/2-\psi)}\left(A_2 + g' A_0 A_1^*\right) \\ &\quad + r'\epsilon e^{i(\delta-\theta/2)}\left(A_1 + g' A_0 A_2^*\right) \end{aligned} \tag{8}$$

where

$$\delta = \frac{\omega_0}{2c}\left(\frac{n}{2}e + \frac{n_1+n_2}{2}l + L\right) + \frac{\zeta_1+\zeta_2}{2}$$

is the mean round-trip phase-shift, and $\theta = (\omega_0/2c)(n_1 - n_2)l + \zeta_1 - \zeta_2$ is the birefringent phase-shift introduced by the non-linear crystal and by the mirrors.

One immediately observes that these equations are not invariant under the gauge transformation $A_1 \longrightarrow A_1 e^{i\varphi}$, $A_2 \longrightarrow A_2 e^{-i\varphi}$, as is the case for the usual equations of a non-degenerate OPO without birefringent mixing. This implies that, unlike in the usual OPO, the phases of the signal and idler amplitudes solutions of equations (8), when they exist, are perfectly determined: phase-locking has occurred between the two oscillating modes, and there is no phase diffusion effect. This phase-locking phenomenon is common to all linearly coupled oscillators [10].

Since the effect of the different elements on the polarization is described by matrices which do not commute, one expects that the system depends on the plate position. However, it is straightforward to show that exchanging the positions of the waveplate and of the crystal amounts to a rotation of $\pi/2$ of the crystal which is equivalent to exchanging indices 1 and 2. This does not change the physics of the system so that we will place ourselves in the case where the waveplate is located after the crystal with respect to the input beam.

Equations (8) have been solved analytically in the small angle regime $\rho \ll 1$ and for small cavity detunings and losses in reference [6].

We will present here the properties of the more complex analytical solutions obtained without any approximations: we will not give the complicated expressions of the solutions, but instead give plots of the most striking results. The exact expressions for the different parameters in the case of a small angle are given in Appendix.

The real and imaginary parts of (8) form a set of two linear equations for the amplitude and phase of the field envelopes A_1, A_2. Thus, one obtains a set of four linear equations with four variables. A non-zero solution of this system exists only when the corresponding 4×4 determinant is zero. This condition gives a real equation for the system parameters, which is fulfilled only in a specific operating range, or *locking zone*, for the self-phase-locked OPO. In the locking zone, this equation has two real solutions for the intracavity pump intensity, corresponding to two possible regimes of the system [5]. In this paper, we will focus our attention to the regime of lower threshold. These solutions give the oscillation threshold for the intracavity pump power as a function of the crystal temperature, the cavity length and the waveplate angle.

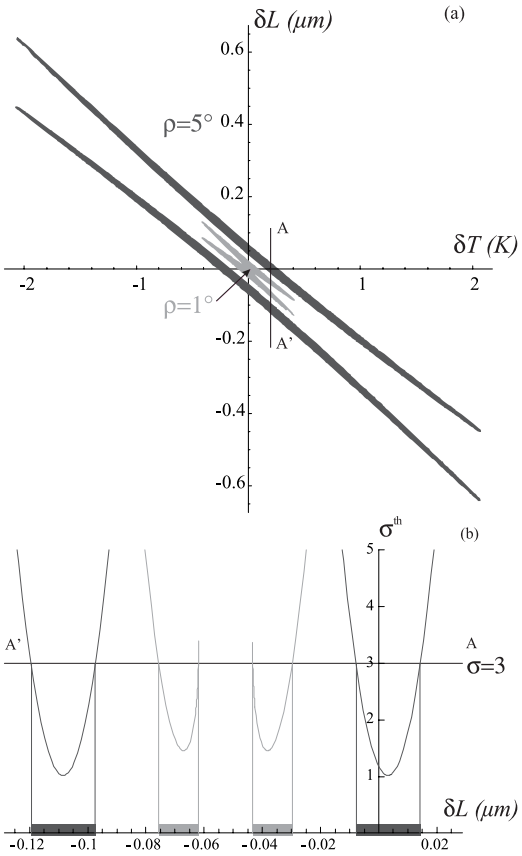

Fig. 3. (a) Locking zone as a function of the cavity length (δL) and of the crystal temperature (δT) for waveplate angle $\rho = 1^\circ$ (light grey) and $\rho = 5^\circ$ (dark grey); $\sigma = 3$. (b) σ^{th} as a function of the cavity length (δL) for $\delta T = 0.2$ K. For $\sigma = 3$, this corresponds to the cross-section AA' of the locking zone. $\Delta\phi = \pi$.

We define σ as the ratio of the intracavity pump power to σ_0 and σ^{th} as the ratio of the intracavity pump power threshold to σ_0. If, for a given set of parameters, σ is larger than σ^{th}, one obtains frequency degenerate oscillation. One can thus plot the values of cavity length and crystal temperature for which σ^{th} is smaller than σ so that there is degenerate oscillation. Figure 3a displays the locking zones for two values of the wave plate angle ρ as a function of $\delta T = T - T_{deg}$ and $\delta L = L - L_{deg}$, where T_{deg} is the temperature for which the exact frequency-degenerate operation occurs without any birefringent coupling and L_{deg} the corresponding cavity resonance length. The locking zone consists of two surfaces which overlap for small values of ρ. Figure 3b shows the cross-section AA' of the locking zone for a given value of δT, that is σ^{th} as a function of δL. All curves in this paper are plotted in the case of KTP for which the index of refraction vary with the following dependence [11]:

$$\frac{dn_1}{dT} = 1.3\times10^{-5}\,\mathrm{K}^{-1} \quad \text{and} \quad \frac{dn_2}{dT} = 1.6\times10^{-5}\,\mathrm{K}^{-1}. \quad (9)$$

Figure 3a shows that the locking zone extension increases as a function of ρ. However, the minimum threshold does not increase with ρ and a threshold equal to the standard OPO threshold can always be found for $\delta T = 0$. For $\delta T \neq 0$, the minimum threshold as a function of δL is no longer equal to one (see Fig. 3, bottom).

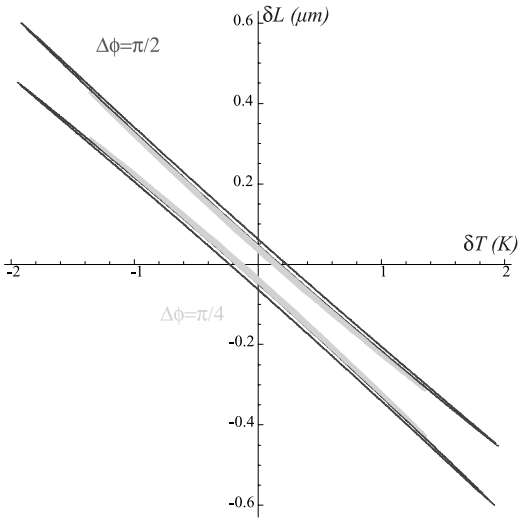

Fig. 4. Locking zone as a function of cavity length and crystal temperature. The thin dark grey line corresponds to a $\lambda/2$ waveplate while the light grey zone corresponds to a $\lambda/4$ waveplate. $\rho = 5^\circ$, $\sigma = 2$.

For a given value of ρ, the coupling parameter $\epsilon = i\sin(\Delta\phi/2)\sin(2\rho)$ is maximized for $\Delta\phi = \pi$ that is for a $\lambda/2$ waveplate. As shown in Figure 4, a different value for $\Delta\phi$ will reduce the locking zone extension but does not change the general shape. In order to maximize ϵ and thus the locking zone extension, one can set $\Delta\phi = \pi$ and $\rho = 45^\circ$. In this case, the locking zone is infinite, in practice only limited by the phase matching.

As the locking zone depends on the temperature, it may be important to take into account the phase matching. However for small values of the waveplate angle, the locking zone extension in δT is small so that the effect of $\Delta k \neq 0$ remains small. As ρ is increased, this effect becomes noticeable and limits effectively the extension of the locking zone to a zone $\delta T \approx 10$ K. We have plotted in Figure 5 σ^{res}, the threshold on resonance: it corresponds to the minimum value of σ as a function of δL for a fixed value of δT. One notices on this figure that σ^{res} is periodic in δT if one does not take into account the phase matching: this is due to the periodicity in temperature of the crystal birefringence. When one takes into account the phase matching, this periodicity disappears (grey curve).

For realistic parameters, such as $R = 90\%$ and $\sigma = 2$, the transverse width of the locking zone is $\Delta L \approx \lambda/\mathcal{F} \approx 10$ nm where $\mathcal{F}$ is the cavity finesse and $\Delta T \approx 50$ mK. These values give the conditions on the length and temperature control loops to remain within the locking zone. These constraints are compatible with the current performances of length and temperature controls.

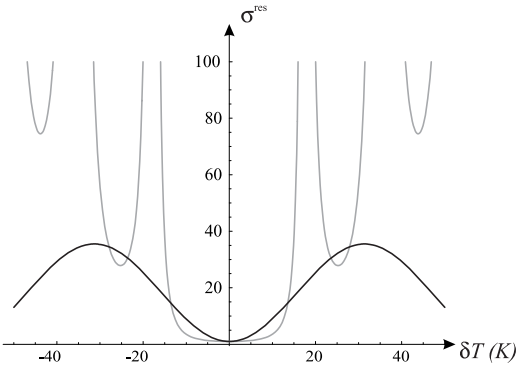

Fig. 5. Normalized threshold on resonance σ^{res} as a function of the temperature for $\rho = 30°$. The black curve corresponds to the result obtained without taking into account the phase matching multiplied by 50 for readability of the figure. The grey curve is plotted taking into account the phase matching.

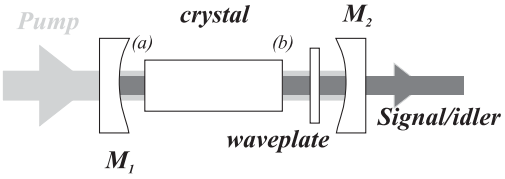

Fig. 6. Set-up of the linear cavity type II OPO.

4 Linear cavity type II OPO

In this section, we study the linear cavity case which is actually used in most experiments. We show here that the linear and ring cavity OPO have different behaviors when one takes into account the reflection phaseshifts on the cavity mirrors for the different interacting waves.

One mirror, M_1 is highly reflective for signal and idler and serves as a coupling mirror for the pump while the other mirror, M_2 is highly reflective for the pump and serves as a coupling mirror for signal and idler (Fig. 6). The phase of the reflection coefficient for signal and idler are taken equal.

We redefine the waveplate coupling constants since the signal and idler beams pass two times in the waveplate[1]:

$$\alpha = \cos(\Delta\phi) + i\sin(\Delta\phi)\cos(2\rho) = \alpha_0 e^{i\psi} \qquad (10)$$

$$\epsilon = i\sin(\Delta\phi)\sin(2\rho) \qquad (11)$$

$\Delta\phi/2$ being replaced by $\Delta\phi$.

As mentioned in the introduction and in the previous section, the linear cavity OPO has distinct features when compared to the ring cavity while the triple resonance does not change the behavior of the system. In the linear cavity the beams undergo two interactions per round-trip. As the phase is important in a parametric interaction the phase-shift between signal and idler and the pump beam between the two nonlinear interactions in the crystal must be taken into account. The equations for the

[1] The free propagation and reflection on the coupling mirror simply shift the two waves by the same phase which does not change the effect of the waveplate.

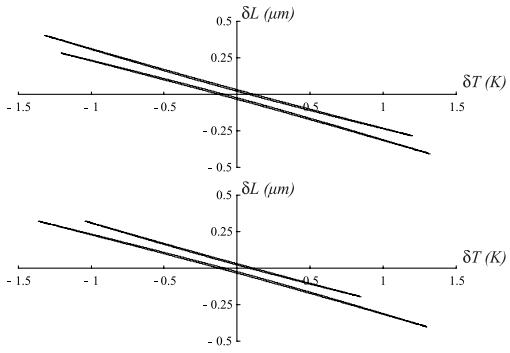

Fig. 7. Locking zone as a function of cavity length and crystal temperature for two values of ξ: top $\xi = 0$, bottom $\xi = \pi/4$. The other values are the same: $\rho = 5°$, $\sigma = 3$.

field envelopes at face (a) of the crystal can be written to the first order in g':

$$\begin{aligned} A_1 &= \alpha_0 r' e^{i(\delta-\delta')}[A_1 + (1+e^{i\xi})g' A_0 A_2^*] \\ &\quad + \epsilon r' e^{i\delta}[A_2 + (1-e^{i\xi})g' A_0 A_1^*] \\ A_2 &= \alpha_0 r' e^{i(\delta+\delta')}[A_2 + (1+e^{i\xi})g' A_0 A_1^*] \\ &\quad + \epsilon r' e^{i\delta}[A_1 + (1-e^{i\xi})g A_0 A_2^*] \end{aligned} \qquad (12)$$

where

$$\delta = \frac{\omega_0}{2c}(2ne + 2\bar{n}l + 2L) + \zeta_1 + \zeta_2 \qquad (13)$$

$$\delta' = \theta - \psi \qquad (14)$$

$$\delta_0 = \frac{\omega_0}{c}(2n_0 l + 2L) + \zeta_0 \qquad (15)$$

$$\xi = \frac{\omega_0}{2c}(2n_0 - 2\bar{n})l - \frac{\omega_0}{c}n(2e) + \zeta_0 - 2\zeta_2 \qquad (16)$$

$2L$ is the total round-trip free propagation length. $\bar{n}$ and θ have been defined in Section 3.

One sees on the first two equations of expression (12) that when the phase-shift ξ is taken equal to 0, the equations are similar to the ring cavity case[2], but with a crystal of double length (factor $2g'$). This is no longer the case when this parameter is changed. A non-zero value of ξ has been shown to increase the threshold of a standard OPO by a significant amount [7]. In the case of a linear cavity with a birefringent element, a dissymmetry appears in the equations due to the terms $1 \pm e^{i\xi}$. Figure 7 shows an example of the results obtained: one notices the dissymmetry between the two locking zones.

Figure 8 presents the value of the threshold on resonance, σ^{res} as a function of the temperature δT and the phase-shift ξ for $\rho = 5°$. One observes that this threshold is no longer obtained for $\delta T = 0$ as is the case for a ring cavity. For small values of ρ and ξ, σ^{res} remains reasonable ($\sigma^{res} < 3$) inside a temperature range of approximately 1 K. This value is small compared to the pure phase matching temperature range of 15 K. However, as ξ

[2] When one neglects the second order term in ϵg if ρ is taken to be small.

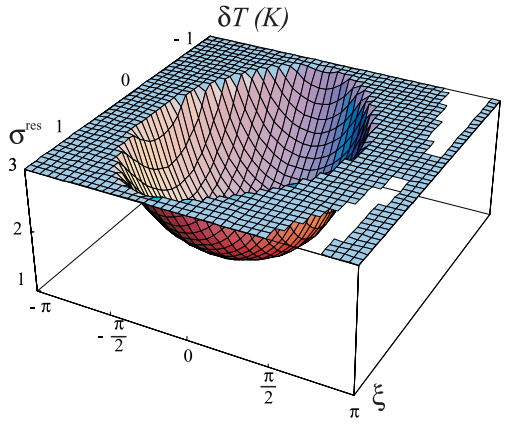

Fig. 8. Normalized threshold on resonance σ_{res} as a function of the crystal temperature δT and of the phase-shift ξ for $\rho = 5°$. Unshaded surfaces correspond to values of $(\delta T, \delta L)$ where frequency degenerate operation is not possible.

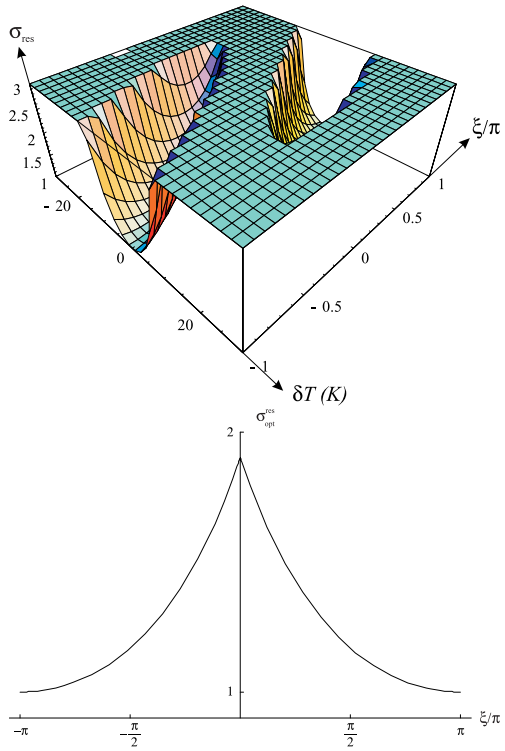

Fig. 9. Normalized threshold on resonance σ_{res} as a function of the crystal temperature δT and of the phase-shift ξ for $\rho = 45°$ (top). Same curve optimized for δT (bottom).

increases and goes to π, σ^{res} diverges: as ξ is fixed by the exact mirror dielectric structure, it is not adjustable experimentally (except by changing the mirrors): this can be a severe limitation to operation of the phase-locked OPO for small values of the waveplate angle ρ.

When ρ is increased, the locking zone size increases and a larger range of temperature can be used with a low threshold. Figure 9 shows the behavior of the normalized threshold on resonance σ_{res} as a function of ξ and δT for $\rho = 45°$. In this case, the minimum value of σ_{res} is obtained for $\xi = \pi$ and $\delta T = 0$. When ξ is lowered to 0, σ_{res} increases. The maximum value of σ_{res} is obtained for $\xi = 0$ and two values of the temperature: it is equal to 1.92 times the standard OPO threshold. This increase by a factor 1.92 is also found for $\xi = \pi$ in the case of the standard OPO [7].

5 Conclusion

We have studied a system composed of an Optical Parametric Oscillator containing a birefringent waveplate inside the optical cavity. As shown previously [5,6], this system allows phase locking of the signal and idler fields. We have obtained equations that are valid for all wave plate angles as well as in different cavity configurations, namely ring or linear cavities. We have shown that the zone where phase locking occurs can be described by the cavity length and the crystal temperature and consists of two zones. As the waveplate angle is increased, the size of the locking zone increases. The optimal configuration is obtained by inserting a $\lambda/2$ waveplate in a ring cavity or a $\lambda/4$ waveplate in a linear cavity with a 45° angle with respect to the crystal's axis. In the case of a ring cavity, the minimum threshold is obtained for a temperature such that the crystal birefringence compensates all the other birefringence in the cavity (waveplate and mirrors) and is equal to the standard OPO threshold. The effect of phase mismatch between the three waves is small for small values of the waveplate angle since the locking zone extension in temperature is small. As ρ is increased, the effect of phase mismatch becomes noticeable and limits in practice the extension of the locking zone. In a linear cavity, the mirrors phase-shift modifies the minimum threshold which becomes dependent on the waveplate angle and can become twice as large as the standard OPO threshold. This increase is known even in standard OPOs but a linear cavity is usually chosen for experimental reasons (losses, mechanical stability...). In both cases (standard and self-phase-locked OPO), this increase is accompanied of a shift in the optimal crystal temperature which may be large and must be taken into account to operate the OPO at low threshold.

Laboratoire Kastler-Brossel, of the École Normale Supérieure and the Université Pierre et Marie Curie, is associated with the Centre National de la Recherche Scientifique. This work was supported by European Community Project QUICOV IST-1999-13071. T. Coudreau is also at the Pôle Matériaux et Phénomènes Quantiques FR CNRS 2437, Université Denis Diderot, 2 place Jussieu, 75251 Paris Cedex 05, France.

Appendix

We give here the exact expression for the lower oscillation threshold in the case of a ring cavity:

$$I^{th} = \frac{u - \sqrt{v}}{g'^2 r'^2} \tag{17}$$

with

$$u = \epsilon^2 + r'^2 - 2r'\alpha_0 \cos(\delta) \cos\left(\frac{\theta}{2} - 2\psi\right) + {\alpha_0}^2 \cos\left(\theta - 2\psi\right) \quad (18)$$

$$v = \left[r'^2 + \epsilon_0^2 - 2r'\alpha_0 \cos(\delta) \cos\left(\frac{\theta}{2} - \psi\right) + \alpha_0^2 \cos^2(\theta - 2\psi)\right]^2 - 1 - r'^4 - 2r'^2\alpha_0^2 - 2r'\left\{r' \cos(2\delta) + \alpha_0\left[r'\alpha_0 \cos(\theta - 2\psi) - 2\left(1 + r'^2\right) \times \cos(\delta) \cos\left(\frac{\theta}{2} - \psi\right)\right]\right\} \quad (19)$$

with the parameters defined in the text.

References

1. R. Graham, H. Haken, Z. Phys. **210**, 276 (1968)
2. J.-Y. Courtois, A. Smith, C. Fabre, S. Reynaud, J. Mod. Opt. **38**, 177 (1991)
3. L. Longchambon, J. Laurat, T. Coudreau, C. Fabre, Eur. Phys. J. D **30**, 287 (2004)
4. J. Mertz, T. Debuisschert, A. Heidmann, C. Fabre, E. Giacobino, Opt. Lett. **16**, 1234 (1991)
5. E.J. Mason, N.C. Wong, Opt. Lett. **23**, 1733 (1998)
6. C. Fabre, E.J. Mason, N.C. Wong, Opt. Comm. **170**, 299 (1999)
7. T. Debuisschert, A. Sizmann, E. Giacobino, C. Fabre, J. Opt. Soc. Am. B **10**, 1668 (1993)
8. L. Longchambon, J. Laurat, T. Coudreau, C. Fabre, in preparation
9. R.C. Jones, J. Opt. Soc. A **31**, 488 (1941)
10. A. Pikovsky, M. Rosenblum, J. Kurths, *Synchronization: A Universal Concept in Nonlinear Sciences* (Cambridge University Press, 2003), ISBN: 052153352X
11. Cristal Laser technical data, Cristal Laser, France